Neurobiology of Disease

Persistent Interneuronopathy in the Prefrontal Cortex of Young Adult Offspring Exposed to Ethanol *In Utero*

Alexander G. J. Skorput, Vivek P. Gupta, Pamela W. L. Yeh, and Hermes H. Yeh

Department of Physiology and Neurobiology, Geisel School of Medicine at Dartmouth, Dartmouth-Hitchcock Medical Center, Lebanon, New Hampshire 03756

Gestational exposure to ethanol has been reported to alter the disposition of tangentially migrating GABAergic cortical interneurons, but much remains to be elucidated. Here we first established the migration of interneurons as a proximal target of ethanol by limiting ethanol exposure *in utero* to the gestational window when tangential migration is at its height. We then asked whether the aberrant tangential migration of GABAergic interneurons persisted as an enduring interneuronopathy in the medial prefrontal cortex (mPFC) later in the life of offspring prenatally exposed to ethanol. Time pregnant mice with *Nkx2.1Cre/Ai14* embryos harboring tdTomato-fluorescent medial ganglionic eminence (MGE)-derived cortical GABAergic interneurons were subjected to a 3 day binge-type 5% w/w ethanol consumption regimen from embryonic day (E) 13.5–16.5, spanning the peak of corticopetal interneuron migration in the fetal brain. Our binge-type regimen increased the density of MGE-derived interneurons in the E16.5 mPFC. In young adult offspring exposed to ethanol *in utero*, this effect persisted as an increase in the number of mPFC layer V parvalbumin-immunopositive interneurons. Commensurately, patch-clamp recording in mPFC layer V pyramidal neurons uncovered enhanced GABA-mediated spontaneous and evoked synaptic transmission, shifting the inhibitory/excitatory balance toward favoring inhibition. Furthermore, young adult offspring exposed to the 3 day binge-type ethanol regimen exhibited impaired reversal learning in a modified Barnes maze, indicative of decreased PFC-dependent behavioral flexibility, and heightened locomotor activity in an open field arena. Our findings underscore that aberrant neuronal migration, inhibitory/excitatory imbalance, and thus interneuronopathy contribute to indelible abnormal cortical circuit form and function in fetal alcohol spectrum disorders.

Key words: binge ethanol; E/I balance; FASD; GABA; *Nkx2.1;* tangential migration

Significance Statement

The significance of this study is twofold. First, we demonstrate that a time-delimited binge-type ethanol exposure *in utero* during early gestation alters corticopetal tangential migration of GABAergic interneurons in the fetal brain. Second, our study is the first to integrate neuroanatomical, electrophysiological, and behavioral evidence that this "interneuronopathy" persists in the young adult offspring and contributes to enduring changes in (1) the distribution of parvalbumin-expressing GABAergic cortical interneurons in the medial prefrontal cortex, (2) GABA-mediated synaptic transmission that resulted in an inhibitory/excitatory synaptic imbalance, and (3) behavioral flexibility. These findings alert women of child-bearing age that fetal alcohol spectrum disorders can be rooted very early in fetal brain development, and reinforce evidence-based counseling against binge drinking even at the earliest stages of pregnancy.

Introduction

Children exposed prenatally to alcohol (ethanol) frequently present with varying degrees of behavioral and cognitive complications that constitute the gamut of fetal alcohol spectrum disorders (FASD) (Astley, 2013). In the United States, 7.6% of pregnant women self-report alcohol use in the last 30 d, and 1.4% self-report episodes of binge drinking. Indeed, binge drinking during pregnancy is particularly risky (Maier and West, 2001), and this is exacerbated by the statistic that, among the 28% of pregnant women that recognize their pregnancy late, the average time to recognition is 10.6 weeks after conception (Ayoola et al., 2009). Thus, a temporal window of susceptibility exists in which

Received April 15, 2015; revised June 11, 2015; accepted July 1, 2015.

Author contributions: A.G.J.S. and H.H.Y. designed research; A.G.J.S., V.P.G., and P.W.L.Y. performed research; A.G.J.S. and H.H.Y. analyzed data; A.G.J.S. and H.H.Y. wrote the paper.

This work was supported in part by Public Health Service Grants R01 AA023410 and R01 MH069826 to H.H.Y.

The authors declare no competing financial interests.

Correspondence should be addressed to Dr. Hermes H. Yeh, Department of Physiology and Neurobiology, Geisel School of Medicine at Dartmouth, Dartmouth-Hitchcock Medical Center, One Medical Center Drive, Lebanon, NH 03756. E-mail: hermes.yeh@dartmouth.edu.

DOI:10.1523/JNEUROSCI.1462-15.2015

 0270-6474/15/3510977-12$15.00/0

the fetus may be exposed to surges of high maternal blood ethanol levels early in gestation, when corticogenesis has begun (Maier and West, 2001; Centers for Disease Control and Prevention, 2012; May et al., 2014).

Ethanol readily crosses the placenta and affects key developmental processes in the fetal brain, including neuronal proliferation and migration (Cuzon et al., 2008; Chang et al., 2012). Notably, exposure of mouse fetuses to ethanol throughout gestation accelerates tangential migration of cortex-bound primordial GABAergic interneurons (Cuzon et al., 2008). An outstanding question is whether disrupted tangential migration is a proximal alteration. We reasoned that, if this effect were proximal, then confining ethanol exposure *in utero* to when corticopetal migration of GABAergic interneurons is most active should suffice to disrupt the normal migratory pattern. To test this hypothesis, we devised an *in vivo* binge-type paradigm of maternal ethanol consumption limited to embryonic day (E) 13.5–16.5, which spans the peak of tangential migration in mouse and approximates mid-first trimester in humans (Clancy et al., 2001). Importantly, human mid-first trimester is also when tangential migration of cortical interneurons peaks (Hladnik et al., 2014). We investigated, in this model of *in utero* ethanol exposure, the migration of embryonic GABAergic cortical interneurons and assessed their long-term neuroanatomical, electrophysiological, and behavioral consequences in young adult offspring.

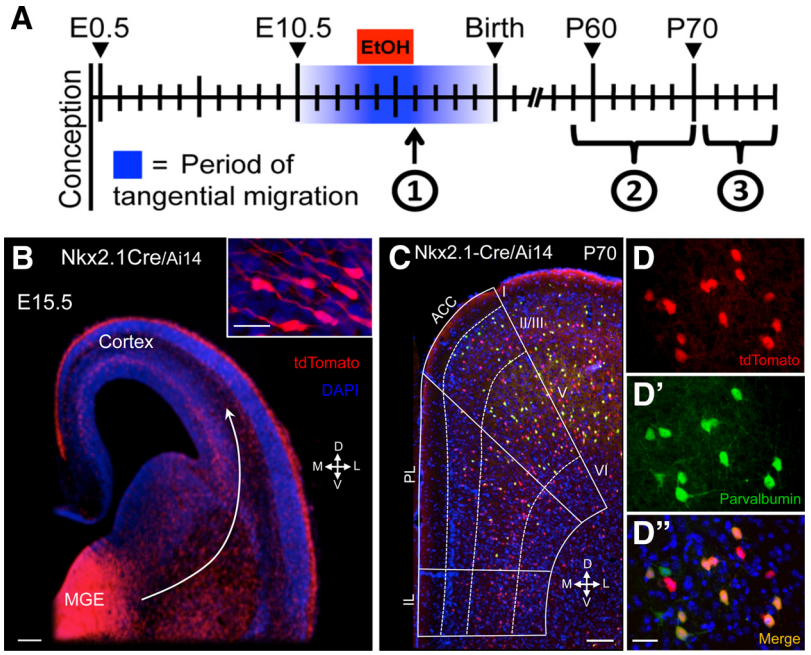

Figure 1. Experimental timeline and tdTomato expression in MGE-derived GABAergic interneurons in the embryonic and young adult brain of *Nkx2.1Cre/Ai14* mice. ***A***, Primordial GABAergic interneurons begin tangential migration from the MGE at ~E10.5. Graded blue area spans the gestational period of active GABAergic interneuron tangential migration, tapering off around birth. The height of migration of MGE-derived GABAergic interneuron migration (E13.5-E16.5) was targeted for binge-type exposure to ethanol (EtOH) by maternal consumption of a liquid diet containing 5% (w/w) ethanol (red bar below time scale): (1) assessment of MGE-derived *Nkx2.1*$^+$ cells in the E16.5 mPFC of *Nkx2.1Cre/Ai14* mice; (2) behavioral testing of reversal learning and open field activity in young adult offspring (P58-P70); and (3) quantification of the number/distribution of MGE-derived GABAergic cortical interneurons and GABA-mediated neurotransmission in the young adult mPFC was assessed in the behaviorally tested mice upon completion of their behavioral testing. tdTomato labels MGE-derived GABAergic interneurons in the embryonic and young adult brain of *Nkx2.1Cre/Ai14* mice. ***B***, Crossing the *Nkx2.1Cre* transgenic mouse with the *Ai14 Cre-reporter* mouse yields *Nkx2.1Cre/Ai14* offspring. An epifluorescence image of a DAPI-counterstained cross section of E15.5 *Nkx2.1Cre/Ai14* mouse brain illustrates tdTomato-fluorescent MGE-derived cortical interneurons that migrate tangentially (white arrow) to reach the cortex. Scale bar, 150 μm. ***C***, Montage showing PV immunostaining in the mPFC of a young adult (P70) *Nkx2.1Cre/Ai14* mouse. Solid lines indicate subregion boundaries based on DAPI-stained cytoarchitecture: ACC, PL, and IL. Dashed white lines indicate cortical layers I, II/III, V, and VI. Scale bar, 175 μm. ***D–D′***, At higher magnification, many of the tdTomato-fluorescent cellular profiles (***D***, red) are also PV-immunoreactive (***D′***, green), confirming the GABAergic interneuronal phenotype of the tdTomato-fluorescent MGE-derived cells (***D″***, orange). Scale bar, 60 μm. Orientation compass: D, Dorsal; V, ventral; M, medial; L, lateral.

In mouse, GABAergic cortical interneurons originate in the medial and caudal ganglionic eminences and the preoptic area. They migrate tangentially over long distances into the cortical anlage, with the peak period of migration between E13.5 and E16.5 (Parnavelas, 2000; Anderson et al., 2001; Marín and Rubenstein, 2001; Jiménez et al., 2002; Batista-Brito and Fishell, 2009; Gelman et al., 2009). The present study was conceived based on the premise that exposure of the fetal brain to ethanol during this peak period disrupts tangential migration. Such disrupted migration may in the long-term contribute to distorting the inhibitory/excitatory (I/E) balance within cortical circuits, resulting in indelible deleterious functional outcomes (Kato and Dobyns, 2005).

Certain transcription factors are expressed in subpopulations of embryonic GABAergic interneurons (Anderson et al., 1997; Lavdas et al., 1999; Xu et al., 2004; Zhao et al., 2008; Long et al., 2009; Flandin et al., 2011). The somatostatin-(SST$^+$) and parvalbumin(PV$^+$)-immunoreactive subpopulations are genetically traced to the *Nkx2.1* lineage originating in the medial ganglionic eminence (MGE) (Xu et al., 2008). We derived the *Nkx2.1Cre/Ai14* mouse line to focus on the MGE-derived PV$^+$ GABAergic cortical interneurons because they exert robust inhibitory influences on pyramidal neurons (Kawaguchi and Kondo, 2002; Kelsom and Lu, 2013; Takada et al., 2014), and because their dysfunction results in I/E imbalance at the circuit level relevant to a number of disorders, including FASD (Gogolla et al., 2009; Lewis et al., 2012; Verret et al., 2012; Sadrian et al., 2013). We focused on the prefrontal cortex (PFC), in particular the medial PFC (mPFC), because it mediates executive function and attentional capacity, both of which are adversely affected by ethanol (Mattson et al., 1999; Bhatara et al., 2006; Ragozzino, 2007; Abernathy et al., 2010; Shaw et al., 2013). We report here that binge-type *in utero* ethanol exposure increases tangentially migrating interneurons in the embryonic mPFC. This proximal effect contributed to enduring neuroanatomical and electrophysiological aberrances in young adult offspring consistent with interneuronopathy-associated synaptic I/E imbalance and demonstration of a PFC-dependent behavioral deficit.

Materials and Methods

Animals. All procedures were performed in accordance with the National Institutes of Health *Guide for the Care and Use of Laboratory Animals* and approved by the Dartmouth Institutional Animal Care and Use Committee. We crossed the *Nkx2.1Cre* transgenic mouse line (originally obtained from Dr. Stewart Anderson; Xu et al., 2008) and the *Ai14 Cre-reporter* mouse (The Jackson Laboratory). For time-pregnant mating, pairs of male and female mice were housed overnight, with the following day designated as E0.5. Embryos and postnatal pups of either sex were included in this study. The day of

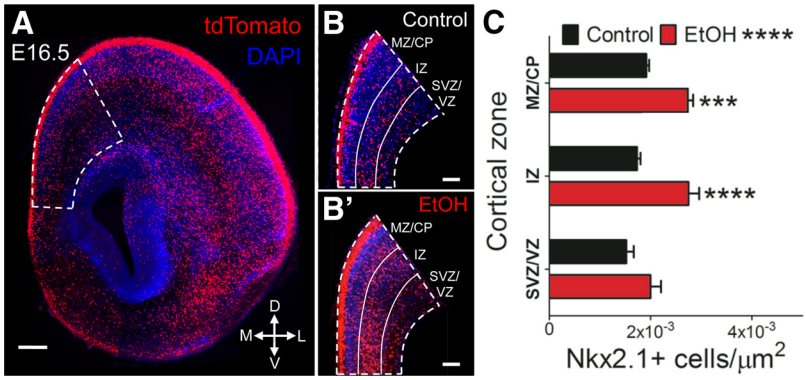

Figure 2. *In utero* binge ethanol exposure during the height of cortical interneuron migration increases MGE-derived interneurons in the embryonic mPFC. ***A***, Cross section of E16.5 *Nkx2.1Cre/Ai14* frontal telencephalon counterstained for DAPI. The dorsomedial telencephalon was outlined as the embryonic mPFC (white dotted line) and analyzed for the number of *Nkx2.1*$^+$ MGE-derived interneurons. Scale bar, 150 μm. ***B***, ***B′***, The ROI in the embryonic mPFC of control (***B***) and ethanol-exposed (***B′***) E16.5 *Nkx2.1Cre/Ai14* embryos (outlined by dashed white lines) was divided into an upper zone, including the MZ/CP, an IZ, and a deep zone including the SVZ/VZ (outlined by solid white lines). Scale bar, 100 μm. ***C***, Quantification of the number of *Nkx2.1*$^+$ cells per square micron stratified into upper (MZ/CP), intermediate (IZ), and deep (SVZ)/(VZ) cortical zones within the ROI. ****$p < 0.0001$ (significant main effect of two-way ANOVA). ***$p < 0.001$ (Bonferroni-corrected *post hoc* analysis by cortical zone). ****$p <$ 0.0001 (Bonferroni-corrected *post hoc* analysis by cortical zone). Orientation compass: D, Dorsal; V, ventral; M, medial; L, lateral.

birth was designated as postnatal day (P) 0. The age range between P58 and P85 was operationally defined to be equivalent to the period of young adulthood.

Binge-type maternal ethanol consumption. We limited the timeframe of *in utero* ethanol exposure from E13.5 to E16.5 to target the height of MGE-derived cortical interneuron migration (see Fig. 1*A*). Pregnant dams were individually housed and assigned to one of two groups: ethanol-fed or control-fed. Mice were maintained under normal 12/12 h light/dark cycle on a liquid diet (Research Diets) supplemented with ethanol (5% w/w; ethanol fed group) or an isocaloric control diet containing maltose (control fed group); water was available *ad libitum*. The liquid food was replenished daily between 3:00 P.M. and 5:00 P.M., when the amount consumed was measured and the dams weighed. Mice were maintained on their respective diets from E13.5 until E16.5, after which they were returned to standard chow. Dam blood alcohol level (80 ± 21 mg/dl) was assessed using a GM7 series analyzer (Analox Instruments), with blood collected via the tail vein at 11:30 P.M. on E15.5. Our regimen of maternal ethanol consumption did not affect litter size (7.50 ± 0.62 control pups; 7.67 ± 0.76 EtOH pups; unpaired *t* test $p > 0.05$).

Immunofluorescence: imaging and analysis. Time-pregnant dams were killed by CO_2 asphyxiation on E16.5, the embryos were quickly removed, their brains dissected, immerse-fixed in PBS containing 4% PFA/0.1 M PBS, and cryoprotected in 30% sucrose/0.1 M PBS. Cryosections (30 μm) were cut with a sliding microtome, mounted on glass slides, DAPI counterstained, and coverslipped with FluorSave Reagent (Calbiochem). For each embryonic brain, 10 consecutive sections were analyzed beginning at equivalent rostral-caudal levels and used for counting tdTomato-fluorescent (*Nkx2.1*$^+$) cells in the embryonic mPFC.

Postnatal mice were transcardially perfused with cold PBS followed by 4% PFA/0.1 M PBS. The brains were removed, immerse-fixed in 4% PFA/0.1 M PBS overnight at 4°C, and cryoprotected. Thirty micrometer coronal cryosections were collected into PBS. For each animal, 10 consecutive sections beginning when all layers of the young adult mPFC are discernible were selected at equivalent rostral-caudal levels and used for counting PV$^+$ interneurons. The sections were blocked for 1 h at room temperature in PBS/10% NGS/0.01% Triton X-100, and incubated overnight at 4°C with mouse anti-parvalbumin primary antibody (1:1000; Millipore). The sections were then incubated overnight at 4°C with AlexaFluor-488 conjugated goat-anti-mouse secondary antibody (1:1000; Millipore). The sections were mounted, counterstained with DAPI, and coverslipped. Negative control with primary antibody omitted was processed in parallel.

Halogen-illuminated epifluorescence images were captured digitally using a 10 × 0.30 NA objective (Olympus) with a CCD camera (Hamamatsu) fitted onto a spinning disk confocal microscope (BX61WI; Olympus) controlled by IPLab version 4.0 software (BD Biosciences). Images were montaged using Fiji (ImageJ) (Preibisch et al., 2009) to yield a full view of the region of interest (ROI). Fiji's auto segmentation algorithm (RenyiEntropy) was used for automated unbiased counting of *Nkx2.1*$^+$ cells in the embryonic mPFC within the manually defined ROI. Cortical zone-specific ROIs were outlined within DAPI-counterstained sections containing the embryonic mPFC. Determining the precise layering with consistency in the embryonic mPFC proved to be difficult. Therefore, we operationally defined three cortical zones to assess the distribution of *Nkx2.1*$^+$ cells without and with *in utero* ethanol exposure: the "upper zone," including the marginal zone (MZ) and cortical plate (CP); the "intermediate zone," equivalent to the intermediate zone (IZ) of the embryonic mPFC; and the "deep zone," including the subventricular zone (SVZ) and ventricular zone (VZ). Images of sections from young adult brains containing the mPFC were captured using a 5 × 0.10 NA objective (Olympus) and montaged. Fiji's manual cell counting tool was used to quantify PV$^+$ interneurons in the young adult mPFC by trained experimenters blinded to the experimental groups to yield unbiased cell counts.

Electrophysiology. Young adult (P70-P80) mice were killed by CO_2 asphyxiation, their brains were dissected and immersed in ice-cold oxygenated (95% O_2, 5% CO_2) cutting solution containing the following (in mM): 3 KCl, 7 $MgCl_2$, 0.5 $CaCl_2$, 1.25 NaH_2PO_4, 28 $NaHCO_3$, 8.3 D-glucose, 110 sucrose, pH 7.4 (adjusted with 1N NaOH). Coronal sections (200 μm) were sliced using a vibrating microtome (Electron Microscopy Sciences) in ice-cold oxygenated cutting solution and then transferred to 32°C oxygenated aCSF containing the following (in mM): 124 NaCl, 5.0 KCl, 2.0 $MgCl_2$, 2.0 $CaCl_2$, 1.25 NaH_2PO_4, 26 $NaHCO_3$, 10 D-glucose, pH 7.4 (adjusted with 1N NaOH) for 30 min. Coronal slices were then maintained in oxygenated aCSF at room temperature for ~60 min before recording.

A brain slice containing the mPFC was transferred to a recording chamber mounted on a fixed-stage upright fluorescence microscope (Olympus BX51WI) equipped with Hoffman Modulation Contrast optics, perfused with oxygenated aCSF (0.5 ml/min), and maintained at 32°C. Layer V pyramidal neurons were identified by their laminar location and morphology, confirmed following filling with AlexaFluor-555 (see Fig. 4*A*). Borosilicate glass patch electrodes (4–6 MΩ in external solution) for recording of GABA-mediated synaptic events were filled with recording solution composed of the following (in mM): 120 KCl, 2.0 $MgCl_2$, 1.0 EGTA, 10 HEPES, 3.0 Mg^{2+} ATP, adjusted to pH 7.3 with 1N KOH). For recording of glutamatergic synaptic events, electrodes were filled with the following (in mM): 100 K-gluconate, 2.0 $MgCl_2$, 1.0 $CaCl_2$, 11 EGTA, 10 HEPES, 30 KCl, 3.0 Mg^{2+} ATP, adjusted to pH 7.3 with 1N KOH. Whole-cell recordings used an AxoPatch 700B amplifier (Molecular Devices). Membrane currents were digitized online at 11 kHz (Digidata1320A; Molecular Devices), recorded with low-pass filtering at 10 kHz, and analyzed offline following low-pass filtering at 100 Hz (Clampfit version 9.0, Molecular Devices). Synaptic currents were recorded at a holding potential of −75 mV. To isolate GABA-mediated postsynaptic currents, CNQX (20 μM) and APV (20 μM) were included in the perfusion solution. To isolate glutamatergic postsynaptic currents, bicuculline (20 μM) was included in the perfusion solution. In experiments that isolated miniature IPSCs (mIPSCs), the CNQX/APV perfusion solution was supplemented with 1 μM TTX to suppress action potential-driven syn-

aptic activity. Spontaneous and miniature synaptic events were analyzed using MiniAnalysis version 6.0 software (Synaptosoft).

Synaptic inputs were evoked by perisomatic stimulation using a bipolar stimulating electrode placed ~100 μm from the cell being recorded. The bipolar stimulating electrode, inserted into an aCSF-filled borosilicate glass pipette with an opening of ~5 μm, delivered the minimum stimulus intensity required to obtain a reliable and reproducible response. Solutions of bath, without or with synaptic blockers (20 μM bicuculline or 20 μM CNQX/APV), were delivered via regulated pressure (<3 psi) through separate barrels of a multibarrel drug pipette assembly placed in the vicinity of the cell (~10 μm). The mean current elicited over the course of bath or drug application was used for analysis. Bicuculline- and CNQX/APV-sensitive currents were computed by subtracting the mean residual current recorded during antagonist applications from the mean current of the baseline recording epochs. Any cell showing a >30% change in total current elicited in the presence of bath alone over the course of the experiment was excluded from analysis (2 control cells, 2 EtOH cells).

Modified Barnes maze and open-field testing. The modified Barnes maze was performed on young adult mice (P58-P70) as previously reported (Koopmans et al., 2003). As illustrated in Figure 8, the maze consisted of 12 equally spaced holes around the circumference of a circular wall (d = 95 cm), with spatial cues (large red letters) separating the holes. Each mouse was randomly assigned an escape hole within a quadrant. All other holes were plugged. Mice were trained to find the escape hole with four 4 min trials per day for 4 consecutive days. Each trial ended when the mouse entered the escape hole. The mouse was then returned to its home cage (escape reinforcement). Following the training phase, the mice were given 2 d off and then tested for their ability to recall the position of the escape hole for 2 d, with four 4 min trials per day (testing phase). After 2 d of testing, the location of the escape hole was switched to the location directly opposite its initial position (reversal phase). Mice were then tested for their ability to find the reversed escape hole with four 4 min trials per day over the subsequent 2 d.

At the beginning of each trial, the mouse was placed in the center of the maze and covered with a start box; time began when the box was removed. Latency to enter escape hole, time per quadrant, home (H), clockwise (CW), opposite (Opp.), counter clockwise (CCW) (clock directions are relative to escape quadrant) (see Fig. 8), and distance per quadrant measurements were made via video tracking software (Videomex-one, Colburn Instruments), running an overhead camera hung at a set distance from the surface of the maze. During a trial, errors made (nose-pokes in nonescape hole) and their locations were recorded manually by observers on opposite sides of the arena.

For open-field testing, young adult mice were allowed to explore for 30 min a novel, moderately lit open-lid clear Plexiglas open field arena (25 × 25 cm; Colburn Instruments) with virtually demarcated activity zones (see Fig. 9*A*). The Plexiglas chamber was equipped with photobeams and sensors to detect activity and was connected to a computer running TruScan software (Colburn Instruments).

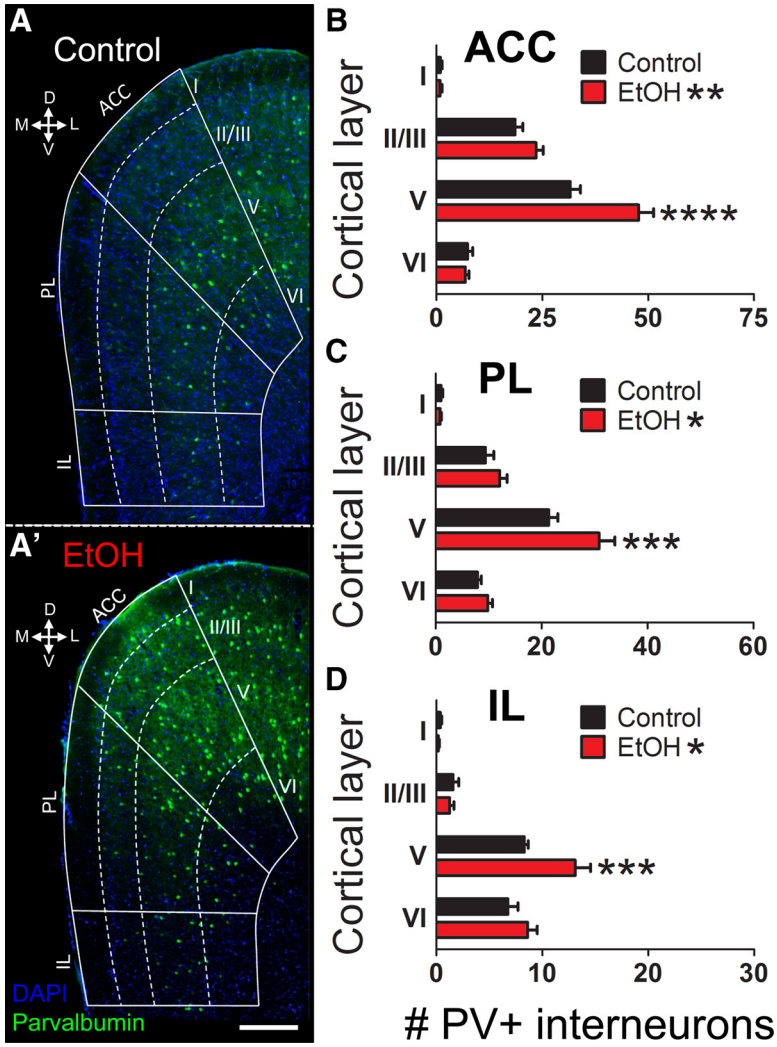

Figure 3. The *in utero* ethanol-induced enhancement of MGE-derived interneurons in the embryonic mPFC persists into adulthood. ***A***, ***A′***, DAPI-counterstained fluorescent image of PV^+ cells in the mPFC of control (***A***) and *in utero* ethanol exposed (***A′***) young adult offspring. Solid white lines outline the mPFC and its subregions the ACC, PL, and IL. In the mPFC, dashed lines outline the cortical layers I, II/III, V, and VI. Scale bar, 300 μm. Counts of PV^+ interneurons by cortical layer in the ACC (***B***), PL (***C***), and IL (***D***) of control (black bars) and ethanol-exposed (red bars) offspring. *$p < 0.05$ (significant main effect of two-way ANOVA). **$p < 0.01$ (significant main effect of two-way ANOVA). ***$p < 0.001$ (Bonferroni-corrected *post hoc* analysis by cortical layer). ****$p < 0.0001$ (Bonferroni-corrected *post hoc* analysis by cortical layer). Orientation compass: D, Dorsal; V, ventral; M, medial; L, lateral.

Following behavior testing, male and female young adult mice were randomly assigned to the neuroanatomical and electrophysiological procedures described above.

Statistics. All histological data were acquired within the ROI from 10 30 μm tissue sections per animal (n = 1: 1 animal = 10 sections). For comparisons of group data obtained from electrophysiological experiments, n refers to the number of cells recorded. The electrophysiological data were also analyzed using the mean data for all cells from an individual animal, with the number of animals as the n value. This analysis revealed that all differences reported using the number of cells as n remained significant. As the variability (SD) of all electrophysiological endpoints was larger between cells than between animals within a given treatment group, we reported the mean data per cell ± SE. Overall, reporting the more variable unit of determination is more representative of the true biological variability (Brien et al., 2006).

All groups consisted of data acquired from a minimum three individual animals from a minimum of three litters. Group means were compared by unpaired t test or two-way ANOVA with Bonferroni post-test as indicated, and reported as mean ± SE.

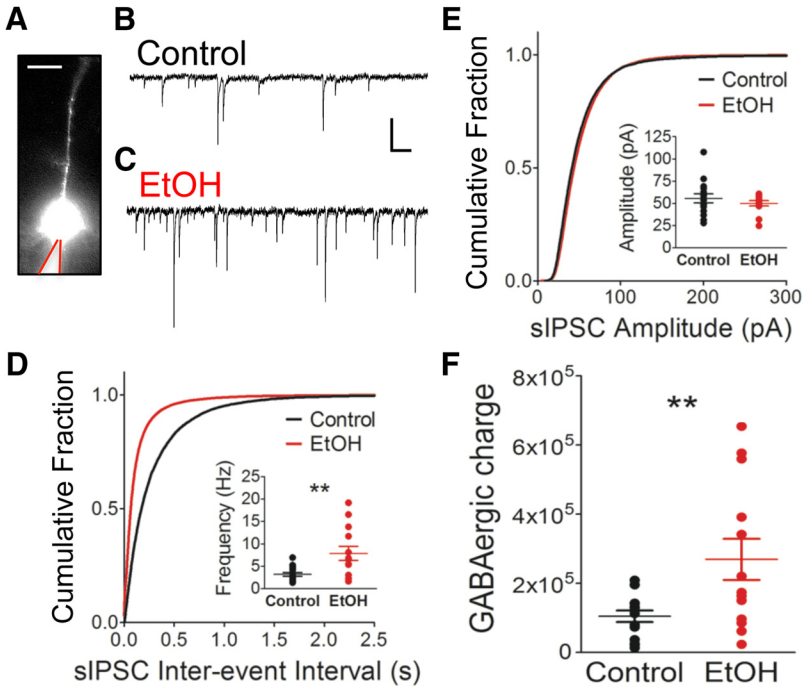

Figure 4. *In utero* ethanol exposure increases spontaneous inhibitory synaptic input to layer V pyramidal neurons in the mPFC of young adult offspring. ***A–C***, sIPSCs were recorded from layer V pyramidal neurons identified morphologically by intracellular filling with AlexaFluor-555 in the mPFC of control (***B***) and ethanol-exposed (***C***) young adult offspring. Scale bar: ***A***, 10 μm. Calibration: ***B***, ***C***, vertical, 50 pA; horizontal, 200 ms. ***D***, Cumulative distribution of sIPSC inter-event intervals recorded from control (black line) and ethanol-exposed (red line) offspring. Inset, Mean frequency of sIPSCs recorded from layer V pyramidal neurons in the PFC of control (black dots) and ethanol-exposed (red dots) offspring. ***E***, Cumulative distribution of sIPSC amplitudes recorded from control (black line) and ethanol-exposed (red line) offspring. Inset, Mean amplitude of sIPSCs recorded from layer V pyramidal neurons in the mPFC of control (black dots) and ethanol-exposed (red dots) offspring. ***F***, Mean GABAergic charge (pA · ms) over the course of the recording epoch in cells recorded from control (black dots) and ethanol-exposed (red dots) offspring. $^{**}p < 0.01$ (unpaired *t* test).

Results

Binge-type ethanol exposure *in utero* during the height of tangential migration enhances entry of MGE-derived interneurons into the embryonic mPFC

We asked whether a binge-type exposure to ethanol *in utero*, delimited to span the height of tangential migration, affected the entry of MGE-derived primordial GABAergic interneurons into the embryonic mPFC. As schematically illustrated in Figure 1*A*, corticopetal migration of the MGE-derived GABAergic interneurons begins at ~E10.5 and tapers off around birth (blue bar with bilateral gradient), with peak activity occurring between E13.5 and E16.5. Therefore, this 3 day gestational time span was targeted for maternal ethanol consumption (Fig. 1*A*, red bar).

In rodent, many conventional markers that aid in identifying subpopulations of GABAergic interneurons in the adult cortex, notably PV and SST that mark the MGE-derived contingent (Rudy et al., 2011), are not expressed reliably until after the second postnatal week. The *Nkx2–1* homeobox gene is prominently expressed in the MGE, and its product the transcription factor Nkx2.1 is required for specification of the cortical interneuron subpopulations that express PV or SST (Xu et al., 2004). Thus, to genetically label MGE-derived interneurons, we crossed *Nkx2.1Cre* transgenic mice with *Ai14 Cre-reporter* mice to yield the *Nkx2.1Cre/Ai14* reporter line that harbors tdTomato-fluorescent *Nkx2.1*$^{+}$ cells (Fig. 1*B*). Cre recombination-based expression of the reporter in the MGE can be seen by E13.5, the earliest gestational day examined (data not shown), in agreement with reports of expression as early as E10.5 (Xu et al., 2008). Figure 1*B* was taken from a coronal section of a hemisected E15.5 *Nkx2.1Cre/Ai14* brain to illustrate *Nkx2.1*$^{+}$ cells concentrated in the MGE, as well as those that have exited the MGE or have migrated tangentially into the developing cortex (Fig. 1*B*, arrow). At a higher magnification, *Nkx2.1*$^{+}$ cells display morphology typical of migrating cells, with a prominent leading process and a short trailing process (Fig. 1*B*, inset). Figure 1*C* illustrates in the young adult mPFC (P70) that a subpopulation of the *Nkx2.1*$^{+}$ cells expresses PV, consistent with them being of MGE origin. The colocalization of PV in *Nkx2.1*$^{+}$ cells is seen to better advantage at higher magnification (Fig. 1*D–D″*).

In light of the PFC-dependent behavioral symptoms that hallmark FASD (Mattson et al., 1999; Kodituwakku et al., 2001; Rasmussen, 2005; Riley and McGee, 2005; Schonfeld et al., 2006; Green et al., 2009; Riley et al., 2011), and functional imaging studies describing altered activation of the frontostriatal circuit in children with FASD (Fryer et al., 2007; Ware et al., 2015), we focused our investigation on the MGE-derived interneurons destined for the mPFC. By E16.5, MGE-derived *Nkx2.1*$^{+}$ cells have reached the embryonic mPFC (Fig. 2*A*). For consistency, and to minimize variability among equivalent histological sections analyzed, the area of the embryonic mPFC enclosed by the dotted white lines in Figure 2*A* was operationally delineated as the ROI and used for counting *Nkx2.1*$^{+}$ cells for all sections. Figure 2*B*, *B′* illustrates enlarged images of the ROI in the E16.5 mPFC of a section taken from a control and a binge ethanol-exposed fetus, respectively. As summarized in Figure 2*C*, cell counts derived from such images revealed that, in the cohort exposed to ethanol *in utero*, the density of *Nkx2.1*$^{+}$ cells (counts per unit area within the ROI) was 39% higher in the embryonic mPFC (control, $1.78 \times 10^{-3} \pm 5.90 \times 10^{-5}$ cells/μm^2, 10 brains from 3 litters; EtOH, $2.61 \times 10^{-3} \pm 1.39 \times 10^{-4}$ cells/μm^2, 10 brains from 4 litters; two-way ANOVA main effect, $p < 0.0001$). Bonferroni-corrected *post hoc* analysis of the two-way ANOVA revealed the observed increase to be statistically significant in the upper (MZ+CP: control, $1.92 \times 10^{-3} \pm 5.89 \times 10^{-5}$ cells/μm^2; EtOH, $2.74 \times 10^{-3} \pm 1.02 \times 10^{-4}$ cells/μm^2, $p < 0.001$) and intermediate (IZ: control, $1.74 \times 10^{-3} \pm 6.69 \times 10^{-5}$ cells/μm^2; EtOH, $2.75 \times 10^{-3} \pm 2.12 \times 10^{-4}$ cells/μm^2, $p < 0.0001$) zones of the developing cortex, with no significant increase in the deep zones (SVZ+VZ: control, $1.52 \times 10^{-3} \pm 1.48 \times 10^{-4}$ cells/μm^2; EtOH, $2.00 \times 10^{-3} \pm 2.48 \times 10^{-4}$ cells/μm^2, $p > 0.05$). These changes were seen without any difference in the total area of the embryonic mPFC or its individual cortical zones (control, $4.23 \times 10^5 \pm 2.72 \times 10^4$ μm^2; EtOH, $3.96 \times 10^5 \pm 2.89 \times 10^4$ μm^2; two-way ANOVA, $p > 0.05$). Thus, by using the gestational stage-delimited paradigm of binge-type ethanol exposure *in* utero, our findings were consistent with a disrupted pattern of tangential migration of GABAergic interneurons into the embryonic mPFC being a proximal effect of ethanol exposure *in utero*.

Binge-type ethanol exposure *in utero* results in more MGE-derived GABAergic interneurons in the young adult mPFC

We next asked whether the increased density of *Nkx2.1*$^+$ cells in the embryonic mPFC persisted as an altered distribution of MGE-derived GABAergic cortical interneurons in young adult offspring exposed to ethanol *in utero*. Because of their prominent role in cortical circuit function and their implications in disorders of I/E imbalance, we focused on PV$^+$ GABAergic interneurons that preferentially sort into the deeper cortical layers (Gogolla et al., 2009; Miyoshi and Fishell, 2011; Lewis et al., 2012; Verret et al., 2012; Cho et al., 2015). Figure 3*A* illustrates PV$^+$ cells in the young adult (P70) mPFC of a control brain (top), the majority (53 ± 2.5%) of which resided within layer V, and a brain exposed to ethanol *in utero* from E13.5 to E16.5 (Fig. 3*A*′). We found an overall 35% increase in the number of PV$^+$ cells in the mPFC of young adult offspring that were exposed to ethanol *in utero*, and this was reflected relatively uniformly in the mPFC subregions of anterior cingulate cortex (ACC, Fig. 3*B*; control, 58.6 ± 3.3 cells; EtOH, 79.1 ± 3.9 cells; two-way ANOVA main effect, $p < 0.01$), prelimbic cortex (PL, Fig. 3*C*; control, 39.6 ± 3.3 cells; EtOH, 53.6 ± 4.7 cells; two-way ANOVA main effect, $p < 0.05$), and infralimbic cortex (IL, Fig. 3*D*; control, 4.3 ± 0.4 cells; EtOH, 5.8 ± 0.6 cells; two-way ANOVA main effect, $p < 0.05$). Bonferroni-corrected *post hoc* analysis by cortical layer revealed an overall increase of 52% in layer V of the mPFC, with an increase of 51% in the ACC (control, 31.6 ± 2.4 cells; EtOH, 47.7 ± 3.5 cells, $p < 0.0001$), 47% in the PL (control, 21.3 ± 1.8 cells; EtOH, 30.9 ± 3.0 cells, $p < 0.001$), and 58% in the IL (control, 8.3 ± 0.4 cells; EtOH, 13.1 ± 1.5 cells, $p < 0.001$). Thus, the increase was layer-specific but not mPFC subregion-selective. Overall, our results provided evidence that changes in the migration of MGE-derived GABAergic interneurons induced by binge-type ethanol exposure *in utero* persist into adulthood. Thus, we postulated that GABA-mediated neurotransmission and cortical circuit function would be altered commensurately in the young adult mPFC.

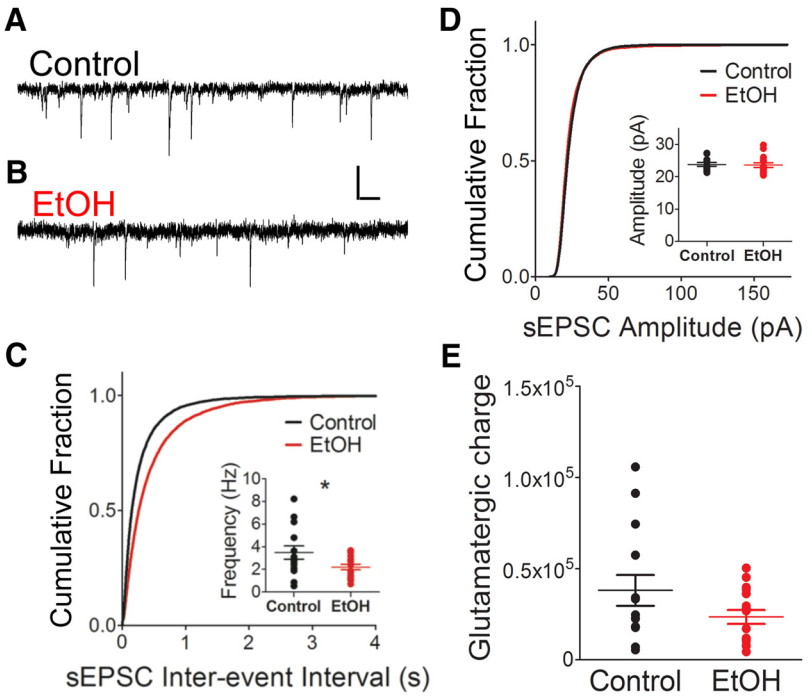

Figure 5. *In utero* ethanol exposure decreases spontaneous excitatory synaptic input to layer V pyramidal neurons in the mPFC of young adult offspring. ***A***, ***B***, sEPSCs were recorded from layer V pyramidal neurons in the PFC of control (***A***) and ethanol-exposed (***B***) young adult offspring. Calibration: ***A***, ***B***, vertical, 20 pA; horizontal, 200 ms. ***C***, Cumulative distribution of sEPSC inter-event intervals obtained from control (black line) and ethanol-exposed (red line) offspring. Inset, Mean frequency of sEPSCs recorded from layer V pyramidal neurons in the mPFC of control (black dots) and ethanol-exposed (red dots) offspring. ***D***, Cumulative distribution of sEPSC amplitudes recorded from control (black line) and ethanol-exposed (red line) offspring. Inset, Mean amplitude of sEPSCs recorded from layer V pyramidal neurons in the mPFC of control (black dots) and ethanol-exposed (red dots) offspring. ***E***, Mean glutamatergic charge (pA · ms) over the course of the recording epoch in cells recorded from control (black dots) and ethanol-exposed (red dots) offspring. *$p < 0.05$ (unpaired *t* test).

Young adult mice exposed to ethanol *in utero* exhibit an I/E imbalance that favors synaptic inhibition in the mPFC

We performed whole-cell patch recording experiments under voltage clamp on layer V pyramidal neurons because they are the principle conduit for efferent information, are robustly innervated and inhibited by GABAergic cortical interneurons, including the PV$^+$ subpopulation, and orchestrate synaptic integration to summate intracortical circuitry (Zhang, 2004; Larkum et al., 2009; Otsuka and Kawaguchi, 2009; Fish et al., 2013). Prefrontal cortical layer V pyramidal neuron identity was confirmed morphologically via filling of the cell with AlexaFluor-555 (Fig. 4*A*). Their spontaneous IPSC events, isolated in the presence of 20 μM CNQX/APV, were monitored in acute slices of the mPFC from control (Fig. 4*B*) and *in utero* ethanol-exposed (Fig. 4*C*) young adult offspring. Analysis of the spontaneous IPSCs (sIPSCs) revealed a distinct leftward shift in the cumulative frequency distribution that reflected a decrease in the inter-event interval (Fig. 4*D*) commensurate with a significant 2.2-fold increase in the mean sIPSC frequency in cells recorded from ethanol-exposed offspring (Fig. 4*D*, inset; control, 3.20 ± 0.39 Hz, 16 cells from 4 offspring from 4 litters; EtOH, 7.87 ± 1.60 Hz, 13 cells from 3 offspring from 3 litters; unpaired *t* test, $p < 0.01$). However, sIPSC amplitude was unaltered by our *in utero* ethanol exposure model as demonstrated by overlapping cumulative distributions of sIPSC amplitudes recorded from control and *in utero* ethanol-exposed offspring (Fig. 4*E*), and no significant difference in the mean amplitude of sIPSCs (Fig. 4*E*, inset; control, 55.7 ± 4.9 pA; EtOH, 50.1 ± 2.9 pA; unpaired *t* test, $p > 0.05$). Overall, the increase in frequency accounted for a 2.2-fold enhancement of the summed integral of sIPSC charge transfer (pA · ms) over the course of the 4 min epoch used to analyze synaptic events (Fig. 4*F*; control, $1.05 \times 10^5 \pm 1.67 \times 10^4$ pA · ms; EtOH, $2.69 \times 10^5 \pm 5.94 \times 10^4$ pA · ms; unpaired *t* test, $p < 0.01$).

By contrast, analysis of the spontaneous EPSCs (sEPSCs) recorded in the presence of 20 μM bicuculline from mPFC pyramidal neurons of control (Fig. 5*A*), and ethanol-exposed offspring (Fig. 5*B*) uncovered a 37% decrease in sEPSC frequency. This was demonstrated by a rightward shift of the cumulative distribution of sEPSC inter-event intervals recorded from *in utero* ethanol-exposed offspring, relative controls (Fig. 5*C*), and a decrease in mean sEPSC frequency (Fig. 5*C*, inset; control, 3.48 ± 0.59 Hz, 14 cells from 3 offspring from 3 litters; EtOH, 2.20 ± 0.25 Hz, 16 cells from 3 offspring from 3 litters; unpaired *t* test, $p = 0.047$).

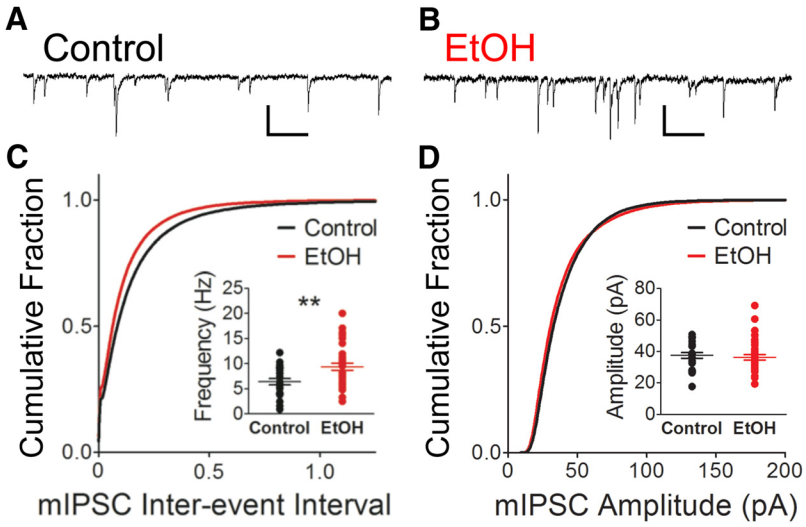

Figure 6. *In utero* ethanol exposure decreases miniature inhibitory synaptic input to layer V pyramidal neurons in the mPFC of young adult offspring. ***A***, ***B***, Miniature IPSCs were recorded from layer V pyramidal neurons in the PFC of control (***A***) and ethanol-exposed (***B***) young adult offspring. Calibration: ***A***, ***B***, vertical, 50 pA; horizontal, 200 ms. ***C***, Cumulative distribution of mIPSC inter-event intervals recorded from control (black line) and ethanol-exposed (red line) offspring. Inset, Mean frequency of mIPSCs recorded from layer V pyramidal neurons in the mPFC of control (black dots) and ethanol-exposed (red dots) offspring. ***D***, Cumulative distribution of mIPSC amplitudes recorded from control (black line) and ethanol-exposed (red line) offspring. Inset, Mean amplitude of mIPSCs recorded from layer V pyramidal neurons in the mPFC of control (black dots) and ethanol-exposed (red dots) offspring. $^{**}p < 0.01$ (unpaired *t* test).

The mean amplitude of sEPSCs recorded from control and ethanol-exposed offspring were not significantly different (Fig. 5*D*, inset; control, 23.8 ± 0.6 pA; EtOH, 23.6 ± 0.7 pA; unpaired *t* test, $p > 0.05$) as demonstrated by overlapping cumulative distributions of sEPSC amplitudes recorded from control and *in utero* ethanol-exposed offspring (Fig. 5*D*). Despite the decrease in sEPSC frequency seen in the *in utero* ethanol-exposed cohort no difference was found in the summed integral of sEPSC charge transfer for the recording epoch (Fig. 5*E*; control, $3.81 \times 10^4 \pm 8.46 \times 10^3$ pA · ms; EtOH, $2.35 \times 10^4 \pm 3.79 \times 10^3$ pA · ms; unpaired *t* test, $p > 0.05$), likely due to a combination of the large variability and overall relatively low frequency of sEPSCs.

The above results suggested the existence of an I/E imbalance in the mPFC of young adults exposed *in utero* to ethanol that was most likely due to presynaptic mechanisms underlying a net strengthening of the inhibitory driving force. This, coupled with increased PV^+ layer V GABAergic interneurons, led us to hypothesize an increase in the number of inhibitory synapses onto PFC layer V pyramidal neurons of young adult offspring exposed to ethanol *in utero*. To physiologically assess inhibitory synapse number, we compared spontaneous mIPSCs in PFC layer V pyramidal neurons of young adult control (Fig. 6*A*) and *in utero* ethanol-exposed mice (Fig. 6*B*). In Figure 6*C*, the inter-event interval cumulative distribution plot and the frequency histogram (inset) both illustrate a significant 1.5-fold increase in the mean frequency of mIPSCs recorded in pyramidal neurons from ethanol-exposed offspring (control, 6.41 ± 0.63 Hz, 23 cells from 3 offspring from 3 litters; EtOH, 9.36 ± 0.71 Hz, 34 cells from 3 offspring from 3 litters; unpaired *t* test, $p < 0.01$). Consistent with our quantification of sIPSC amplitude, no change was seen in mIPSC amplitude between groups (Fig. 6*D*, inset; control, 37.5 ± 1.8 pA; EtOH, 36.28 ± 1.8 pA; unpaired *t* test, $p > 0.05$) as demonstrated by overlapping cumulative distributions of mIPSC amplitudes recorded from control and *in utero* ethanol-exposed offspring (Fig. 6*D*). Thus, the effects of accelerated tangential migration and increased GABAergic interneurons in the embryonic mPFC persists into young adulthood as an overall enhanced inhibitory synaptic drive onto layer V pyramidal neurons. Such an enhancement could be accounted for by (1) more MGE-derived interneurons innervating a pyramidal neuron, (2) each interneuron contributing more inhibitory synapses, and (3) increased probability of GABA release at presynaptic sites, or any combination of the above.

In another series of electrophysiological experiments, we asked whether *in utero* ethanol exposure commensurately shifted synaptic I/E balance toward inhibition when assessed within individual layer V pyramidal neurons by quantifying the I/E ratio of evoked synaptic responses. Figure 7*A* illustrates the experimental setup, with a patch-recording pipette placed on the soma of a layer V pyramidal neuron and a multibarrel drug pipette navigated to its vicinity. Perisomatic stimulation evoked compound inhibitory and excitatory synaptic current responses that could be pharmacologically discerned with focal application of bicuculline ($GABA_A$ receptor antagonist; 20 μM) or CNQX/APV (AMPA and NMDA receptor antagonist, respectively; each 20 μM). As illustrated in Figure 7B_1, subtracting the mean evoked current response recorded in the presence of bicuculline (gray trace) from the mean evoked current in the presence of bath alone (black trace) revealed the GABA-mediated component of the synaptically evoked compound current response (red trace) in this pyramidal neuron. In the same cell (Fig. 7B_2), subtracting the mean evoked current response monitored in the presence of CNQX/APV (gray trace) from the mean baseline evoked current (black trace) uncovered the glutamatergic component (red trace). Thus, the proportion of the total charge carried by the mean baseline evoked synaptic response belonging to the inhibitory and excitatory fractions was used to assess the ratio of I/E balance for a given pyramidal neuron. Figure 7*C* illustrates the mean charge of the evoked current (eQ) recorded overtime in the presence of bath or synaptic blockers from control (black line and symbols) and ethanol-exposed (red line and symbols) offspring. Analysis of the bicuculline-sensitive current showed the GABA-mediated fraction to be 25% greater in mPFC layer V pyramidal neurons recorded from young adult mice that had been exposed to ethanol *in utero* (Fig. 7*D*; control, 59.0 ± 3.0%, 12 cells from 3 offspring from 3 litters; EtOH, 73.4 ± 3.3%, 10 cells from 4 offspring from 3 litters; unpaired *t* test, $p < 0.01$). In addition, the absolute value of the GABAergic charge elicited by perisomatic stimulation was larger in the mPFC of young adult mice exposed to ethanol *in utero* relative to controls (control, 5521 ± 859 pA · ms, 12 cells from 3 offspring from 3 litters; EtOH, 8312 ± 601 pA · ms, 10 cells from 4 offspring from 3 litters; unpaired *t* test, $p < 0.05$), with no difference in whole-cell capacitance (control, 41.14 ± 2.89 pF; EtOH, 40.45 ± 3.57 pF; unpaired *t* test, $p > 0.05$), resting membrane potential (control, −65.5 ± 1.43 mV; EtOH, −66.4 ± 1.03 mV; unpaired *t* test, $p > 0.05$), or input resistance (control, 143.7 ± 8.8 MΩ; EtOH, 146.2 ± 12.5 MΩ; unpaired *t* test, $p > 0.05$). In contrast, there was no significant difference in the glu-

tamatergic fraction (Fig. 7*E*; control, 19.5 ± 5.8%; EtOH, 8.1 ± 3.3%; unpaired *t* test, $p > 0.05$). We ruled out run-down as a factor because, across all cells, the total charge of the synaptically evoked responses were comparable before drug application and after washout (baseline, −11,279 ± 806 pA · ms; final washout, −10,465 ± 783 pA · ms; 22 cells from 7 offspring from 6 litters; paired *t* test, $p > 0.05$). These results provide additional evidence that an enduring outcome of ethanol exposure *in utero* is an I/E imbalance due to increased synaptic inhibition, as observed in the young adult mPFC.

We then asked whether the observed differences in synaptically evoked compound inhibitory and excitatory current responses between the control and ethanol-exposed cohorts led to a change in the ratio of I/E charge. We analyzed data derived from mPFC layer V pyramidal neurons in which compound inhibitory and excitatory stimulus-evoked responses could be clearly discerned ($n = 8$ for control and 7 for ethanol-exposed groups). Of the 22 cells shown in Figure 7*C–E*, data obtained from 4 cells in the control group and 3 cells in the ethanol-exposed group were omitted from analysis either because the excitatory component was absent in the stimulus-evoked synaptic response (3 and 2 cells from control and ethanol-exposed groups, respectively) or because pharmacological isolation of the inhibitory or excitatory components was deemed to be incomplete (1 cell in each group). In Figure 7*E*, the scatter plot illustrating the I/E ratio indicates a nearly 3.0-fold increase in mPFC layer V pyramidal neurons of young adult mice exposed to ethanol *in utero* relative to controls (control, 3.2 ± 0.9, 8 cells from 3 offspring from 3 litters; EtOH, 9.5 ± 2.4, 7 cells from 3 offspring from 3 litters; unpaired *t* test, $p < 0.05$). Simultaneous application of bicuculline, APV, and CNQX blocked 80%–90% of the total evoked synaptic current response. The residual current may be due to mediation by neurotransmitters other than GABA and glutamate, or simply GABA- and/or glutamate-mediated inputs that are too far from the soma to be blocked by focal application of the antagonists. Regardless, because the calculated glutamatergic current represents the difference between the mean baseline and synaptic current response evoked in the presence of CNQX/APV, and the same applies for GABA-mediated synaptic current responses with respect to blockade by bicuculline, our analysis of evoked synaptic inhibition, vis-á-vis excitation, should be devoid of any potentially confounding currents.

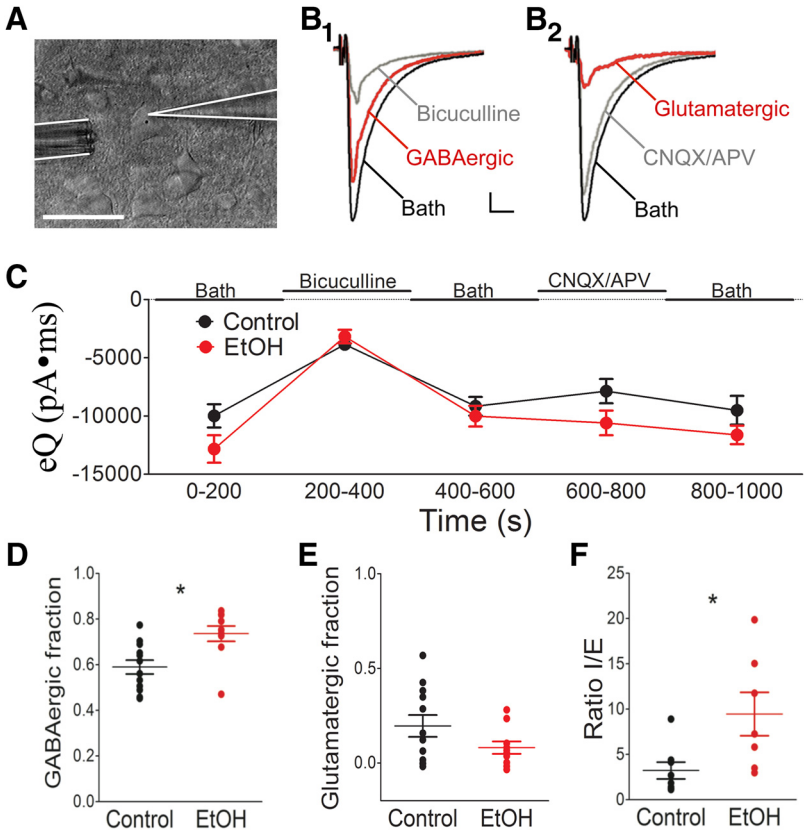

Figure 7. Young adult mice exposed to ethanol *in utero* exhibit an I/E imbalance of locally evoked synaptic input in the mPFC. ***A***, An mPFC layer V pyramidal neuron viewed under Hoffman Modulation Optics being recorded with a patch-clamp recording pipette (outlined on the right) and the multibarrel drug pipette placed in close vicinity (outlined on the left). Scale bar, 30 μm. ***B*$_1$**, The synaptically evoked current monitored in the presence of bicuculline (gray trace) was subtracted from the mean bath current (black trace) to reveal the GABAergic current (red trace). ***B*$_2$**, In the same cell, the synaptically evoked current monitored in the presence of CNQX/APV (gray trace) was subtracted from the mean bath current (black trace) to reveal the glutamatergic current (red trace). Calibration: ***B*$_1$**, ***B*$_2$**, vertical, 200 pA; horizontal, 10 ms. ***C***, Charge of evoked synaptic current responses (eQ) monitored in the presence of bath or synaptic blockers from control (black) and ethanol-exposed (red) plotted as a function of time. ***D***, The GABAergic fraction of mean bath evoked responses recorded from control (red dots) and ethanol-exposed (black dots) mPFC. ***E***, The glutamatergic fraction of mean bath evoked responses recorded from control (red dots) and ethanol-exposed (red dots) mPFC. ***F***, The ratio of GABAergic charge (inhibitory) to glutamatergic charge (excitatory) from control (black dots) and ethanol-exposed (red dots) pyramidal cells exhibiting a compound evoked synaptic response. *$p < 0.05$ (unpaired *t* test).

Young adult offspring exposed to ethanol *in utero* exhibit decreased behavioral flexibility and hyperactivity

The modified Barnes maze is a behavioral task of spatial learning and memory in which mice use visual spatial cues to escape the maze (Fig. 8*A*) (Koopmans et al., 2003). The inclusion of a reversal phase one day following the testing phase (Fig. 8*B*) allows for assessment of reversal learning and behavioral flexibility (Vetreno and Crews, 2012; Fowler et al., 2013). The training and testing phases of the modified Barnes maze are strongly dependent upon the hippocampus; we found no deficits in these phases in either latency to find the escape hole (Fig. 8*C*) or the number of errors, scored as nose-pokes in the nonescape holes (Fig. 8*D*). The reversal phase, on the other hand, depends on proper functioning of the PFC; young adult offspring exposed to ethanol *in utero* were less efficient at running the maze during this phase, as indicated by increased errors/trial (Fig. 8*D*; control, 4.5 ± 0.5 errors, 14 offspring from 4 litters; EtOH, 7.3 ± 0.5 errors, 19 offspring from 4 litters; two-way ANOVA main effect, $p < 0.001$, Bonferroni post test, $p < 0.001$). Analysis of errors on reversal day 1 revealed that ethanol-exposed offspring committed more errors relative to controls (Fig. 8*E*; control, 2.7 ± 0.4 errors; EtOH, 4.8 ± 0.4 errors; two-way ANOVA main effect, $p < 0.001$). Importantly, Figure 8*E* also indicated that the increased errors were committed within the quadrant that housed the original escape hole during the training and testing phases (opposite) (control, 0.92 ± 0.22 errors; EtOH, 1.88 ± 0.15 errors; two-way ANOVA Bonferroni post test, $p < 0.001$). These perseverative-type errors

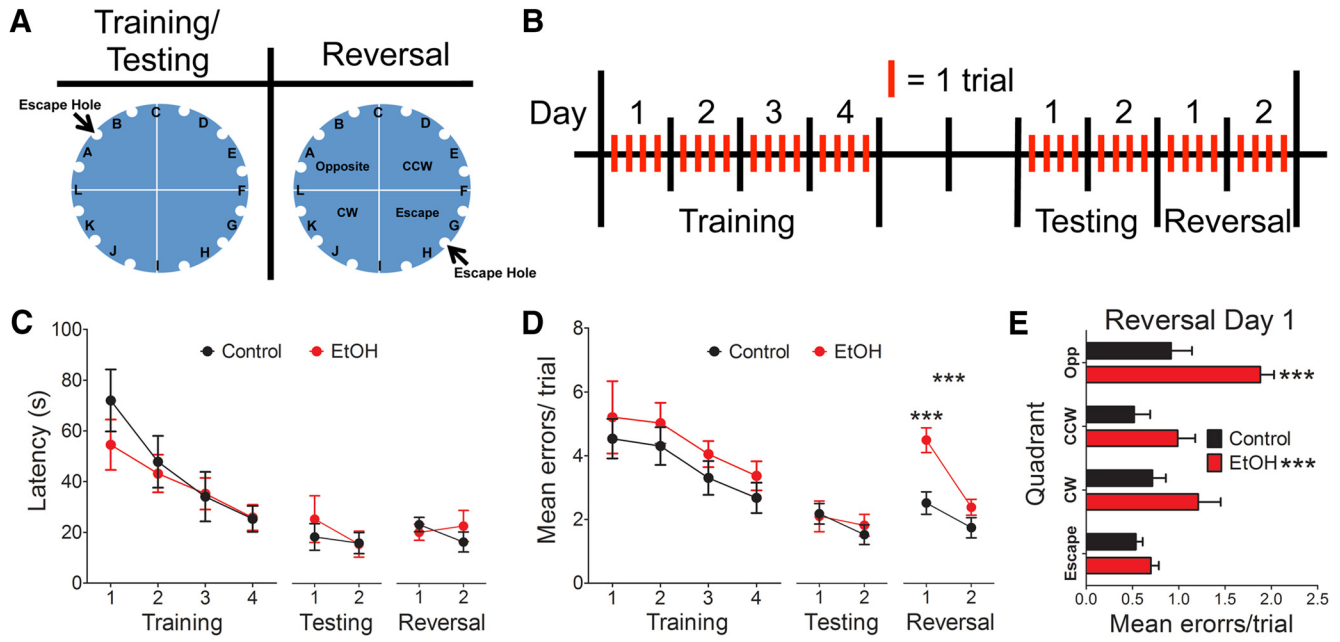

Figure 8. Young adult offspring exposed to ethanol *in utero* exhibit decreased behavioral flexibility. ***A***, ***B***, Over the course of days with multiple trials per day, mice were trained and subsequently tested in the modified Barnes maze to assess their ability to locate the escape hole. Following testing, the location of the escape hole was reversed, and mice were retested for their ability to adapt and efficiently locate the new escape hole. ***A***, Quadrant designations are made relative the location of the escape hole: escape, clockwise (CW), opposite, counterclockwise (CCW). ***C***, Mean latency to locate the escape hole per trial for control (black dots connected with black line) and ethanol-exposed (red dots connected with red line) young adult offspring. ***D***, Mean number of errors committed per trial by control (black dots connected with black line) and ethanol exposed (red dots connected with red line) young adult offspring. ***E***, Mean number of errors committed per trial on reversal day 1 as a function of error location for control (black bars) and ethanol-exposed (red bars) young adult offspring. ***D***, $^{***}p < 0.001$, significant main effect of two-way ANOVA on the reversal phase. ***E***, $^{***}p < 0.001$, significant main effect of two-way ANOVA. Bonferroni-corrected *post hoc* analysis by reversal day D or error quadrant E. $^{***}p < 0.001$.

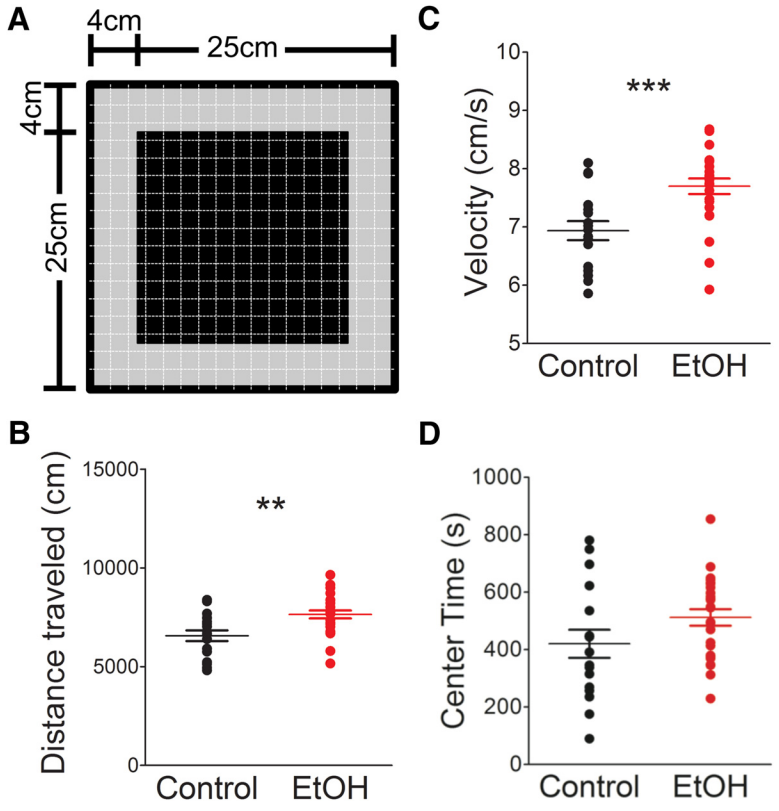

Figure 9. Young adult offspring exposed to ethanol *in utero* are hyperactive. ***A***, The open field layout with black center area and gray margin area. White lines indicate the location of photo beams used to track the animal's position. ***B***, Distance traveled by young adult offspring each given 30 min to explore the 25 cm × 25 cm open field arena. ***C***, Mean velocity of individual movements. ***E***, Time spent in the center area of the arena. $^{**}p < 0.01$ (unpaired *t* test). $^{***}p < 0.001$ (unpaired *t* test).

are indicative of impaired behavioral flexibility (Hunt et al., 1995; Vetreno and Crews, 2012; Fowler et al., 2013).

Latency as a behavioral endpoint derived from the modified Barnes maze needs to be interpreted in light of the locomotor phenotype (O'Leary and Brown, 2013). We therefore assessed locomotor activity in an open field arena demarcated with virtual activity zones (Fig. 9*A*). Young adult mice exposed to ethanol *in utero* exhibited a hyperactive exploratory phenotype in the open-field paradigm, hallmarked by increased total distance traveled (Fig. 9*B*; control, 6568 ± 272 cm, 17 offspring from 4 litters; EtOH, 7641 ± 200 cm, 25 offspring from 5 litters; unpaired *t* test, $p < 0.01$) and velocity of travel (Fig. 9*C*; control, 6.94 ± 0.16 cm/s; EtOH, 7.70 ± 0.13 cm/s; unpaired *t* test, $p < 0.001$). This increase in locomotor activity may explain why the latency times did not increase on reversal day 1, despite the ethanol-exposed mice committing more errors. Further, the increased locomotor activity observed here in mice exposed to ethanol *in utero* was reminiscent of the hyperactivity seen clinically in FASD (Riley et al., 1979, 1986; Schneider et al., 2011). By contrast, the time spent in the center portion of the arena was not significantly different between groups (Fig. 9*D*; control, 420 ± 49 s; EtOH, 512 ±

29 s; unpaired *t* test, $p > 0.05$), suggesting comparable levels of anxiety (Prut and Belzung, 2003).

Discussion

Aberrances in cortical form and function are implicated in behavioral deficits associated with a variety of neurodevelopmental disorders, including impaired executive function and hyperactivity commonly seen in FASD (Bhatara et al., 2006). Although altered I/E balance within the cortical circuit has been proposed to contribute to the neurobehavioral and cognitive deficits in FASD (Sadrian et al., 2013), supportive experimental data are limited. Development of proper I/E synaptic balance requires orchestration of neurogenesis, migration, and integration, and dysfunction of PV^+ GABAergic interneurons results in I/E imbalance within cortical circuits (Gogolla et al., 2009; Lewis et al., 2012; Verret et al., 2012). In this light, we report three major findings regarding the consequences of an early gestational binge-type exposure to ethanol on (1) the migration of MGE-derived GABAergic interneurons to the embryonic mPFC in the short-term, (2) mPFC form and function in the long-term, and (3) enduring deficits in PFC-dependent behavior.

Gestational age-delimited exposure to ethanol alters the normal pattern of tangential migration

Exposure to ethanol *in utero* spanning the height of tangential migration increased the number of MGE-derived GABAergic cortical interneurons in the embryonic mPFC. We interpreted this as a short-term proximal effect of the ethanol exposure accelerating tangential migration. This is consistent with the findings of our previous study in which GABAergic interneurons chronically exposed to ethanol migrated at a faster rate (Cuzon et al., 2008). The present study did not rule out other possibilities, such as binge ethanol *in utero* causing a delayed surge in the proliferation of the MGE-derived cells. A rerouting may have also occurred such that MGE-derived GABAergic interneurons normally destined for other embryonic brain regions, such as the striatum, populate the embryonic mPFC (Marín et al., 2000; Nóbrega-Pereira et al., 2008). These issues call for a comprehensive analysis of the distribution and genesis of cortical and extracortical GABAergic interneurons without or with ethanol exposure *in utero*. We note that, in humans, despite the pallial origin of a large contingent of cortical interneurons, ~35% of them are generated in the subpallium and migrate tangentially to the cortex (Letinic et al., 2002). Thus, an aberrant tangential migration may nonetheless contribute to an enduring interneuronopathy in FASD.

Binge-type exposure to ethanol *in utero* results in persistent changes in cortical form and function

Our results revealed a layer-specific increase of MGE-derived interneurons in the mPFC of young adult offspring subjected to binge ethanol exposure *in utero*. The preferential increase in the number of PV^+ neurons in layer V of the mPFC begs the issues of binge exposure to ethanol *in utero* affecting the sorting of GABAergic interneurons within the cortical layers. In mouse corticogenesis, GABAergic cortical interneurons have similar birthdates and share the same migratory paths and temporal entry into the cortical plate (Miyoshi and Fishell, 2011). Sorting begins early postnatally, with the majority of the initially evenly distributed MGE-derived interneurons translocating to deeper cortical layers (layers V/VI). Within this scheme, the selective increase of PV^+ interneurons in layer V of the *in utero* ethanol-exposed young adult mPFC could reflect their enhanced translocation during early postnatal development. Our findings suggest that the characteristic sorting of MGE-derived interneurons into the deeper cortical layers remains unperturbed.

Of the GABAergic cortical interneurons, the PV^+ and SST^+ subpopulations are of MGE origin, with an ~3:2 ratio, respectively (Rudy et al., 2011). The present study did not address directly the disposition of the SST^+ interneurons in the embryonic and young adult mPFC. However, given that interneurons of the same ganglionic origin tend to be intrinsically programmed in terms of the cortical layers they ultimately populate (Miyoshi and Fishell, 2011), it is reasonable to assume that the disposition of the PV^+ interneurons would also reflect that of the SST^+ interneurons. Future investigations will need to address whether cortical neuronal subpopulations, notably those from the caudal ganglionic eminence and the preoptic area (Xu et al., 2004; Gelman et al., 2009), are differentially affected long-term by ethanol exposure *in utero*.

The functional outcome of an altered disposition of PV^+ interneurons in the young adult mPFC was a net augmentation of GABA-mediated synaptic transmission associated with enhanced I/E ratio, as demonstrated here in layer V mPFC pyramidal neurons. The fast-firing PV^+ and SST^+ Martinotti cells comprise >80% of cortical interneurons in layer V, where they mediate robust GABA-mediated inhibition onto layer V pyramidal cells to regulate pyramidal cell excitability and cortical network activity (Hasenstaub et al., 2005; Haider and McCormick, 2009). Predictably, altering GABA-mediated neurotransmission would compromise the I/E balance of cortical circuits (Kato and Dobyns, 2005; Sadrian et al., 2013). Indeed, MGE-derived internerneurons regulate intracortical inhibition to achieve large-scale pacing of cortical rhythm and, thus, contribute to cognition (Hasenstaub et al., 2005; Haider and McCormick, 2009; Cho et al., 2015). Consistent with the view that FASD is a disorder of I/E imbalance (Sadrian et al., 2013), we propose that the ethanol-induced effect on tangential migration persists into young adulthood as a defect in mPFC neuroanatomical form and circuit function. We propose further that interneuronopathy (Kato and Dobyns, 2005; Price et al., 2009) may contribute to the cortical dysfunction in FASD. Our finding of reduced sEPSCs frequency in mPFC layer V pyramidal neurons points to the need to investigate whether *in utero* ethanol exposure affects the genesis, migration, and integration of radially migrating cells within the dorsal cerebral wall. Such studies will provide a more complete picture of *in utero* ethanol-induced teratogenic outcomes related to corticogenesis and adult circuit function.

Binge exposure to ethanol *in utero* leads to impaired PFC-dependent executive function

We considered whether the observed shift in I/E balance might be associated with persistently impaired PFC function in the behaving young adult mouse. Our behavioral testing revealed a perseverative behavioral deficit in offspring exposed *in utero* to binge-type ethanol. Notably, the young adult mice tested displayed this deficit only on the first day of the reversal phase, suggesting that they are able to adjust to a new situation, albeit less efficiently.

The shift in I/E balance reported in the present study also bears on the operation of cortical circuits in behaving animals. Prefrontal cognitive deficits have been reported in genetic models of cortical GABAergic interneuron dysfunction (Bissonette et al., 2014), as well as following microinjection of $GABA_AR$ agonist in the PFC (Shaw et al., 2013). Of particular relevance to this work, PFC interneurons are functionally involved in coordinated activity during reversal learning (Bissonette et al., 2015), and behav-

ioral inflexibility has been reported to be a consequence of their dysfunction (Cho et al., 2015). These studies underscore the reliance of PFC-dependent executive function on proper functioning of cortical interneurons and level of GABAergic regulation.

Consistent with our observations, long-term PFC-dependent behavioral deficits in executive function have been reported following gestational ethanol exposure (Marquardt et al., 2014). In addition, the hyperactivity observed in young adult offspring exposed to ethanol *in utero* is consistent with other preclinical studies as well as with clinical observations of patients with FASD (Riley et al., 1979, 1986; Schneider et al., 2011). This hyperactivity does not compromise or account for the behavioral flexibility deficit because, unlike latency, errors as an endpoint are resistant to the confounding effects of disparate locomotor activity (O'Leary and Brown, 2013). At the level of synaptic circuits, although heightened inhibition was the driving force of I/E imbalance in our study, it would have been just as plausible for an imbalance of intracortical circuitry favoring excitation to produce the same behavioral deficits. Indeed, the establishment of the imbalance itself supercedes the direction of I/E imbalance in terms of disrupting proper cortical development and function (Gogolla et al., 2014).

Implications in FASD

The demonstration that a binge-type *in utero* ethanol exposure disrupts the normal pattern of tangential migration is of both conceptual and practical significance. Conceptually, it not only lends credence to our previous study but also underscores that ethanol exposure *in utero*, whether short-term or throughout gestation, can lead to interneuronopathy, broadly defined to include neurodevelopmental disorders that can be attributed at least in part to aberrant migration of GABAergic cortical interneurons (Kato and Dobyns, 2005). In this light, our study proposes that FASD has in common aspects of developmental etiology that are typically associated with other neurodevelopmental disorders hallmarked by a continuum of behavioral and cognitive deficits, most notably autism spectrum disorder, attention deficit hyperactive disorder, and schizophrenia. Practically, because E13.5-E16.5 in mouse cortical development is approximately equivalent to human mid-first trimester (Clancy et al., 2001), our findings alert women of child-bearing age that FASD can be rooted very early in fetal development, and contribute to the scientific database counseling against binge drinking even at early stages of pregnancy. Indeed, human epidemiological and preclinical data are in agreement that binge drinking during pregnancy increases the severity of deleterious outcomes compared with drinking equivalent levels of ethanol over extended periods of time (Maier and West, 2001).

References

Abernathy K, Chandler LJ, Woodward JJ (2010) Alcohol and the prefrontal cortex. Int Rev Neurobiol 91:289–320. CrossRef Medline

Anderson SA, Eisenstat DD, Shi L, Rubenstein JL (1997) Interneuron migration from basal forebrain to neocortex: dependence on Dlx genes. Science 278:474–476. CrossRef Medline

Anderson SA, Marín O, Horn C, Jennings K, Rubenstein JL (2001) Distinct cortical migrations from the medial and lateral ganglionic eminences. Development 128:353–363. Medline

Astley SJ (2013) Validation of the fetal alcohol spectrum disorder (FASD) 4-digit diagnostic code. J Popul Ther Clin Pharmacol 20:e416–e467. Medline

Ayoola AB, Stommel M, Nettleman MD (2009) Late recognition of pregnancy as a predictor of adverse birth outcomes. Am J Obstet Gynecol 201:156.e1–156.e6. CrossRef Medline

Batista-Brito R, Fishell G (2009) The developmental integration of cortical interneurons into a functional network. Curr Top Dev Biol 87:81–118. CrossRef Medline

Bhatara V, Loudenberg R, Ellis R (2006) Association of attention deficit hyperactivity disorder and gestational alcohol exposure: an exploratory study. J Atten Disord 9:515–522. CrossRef Medline

Bissonette GB, Bae MH, Suresh T, Jaffe DE, Powell EM (2014) Prefrontal cognitive deficits in mice with altered cerebral cortical GABAergic interneurons. Behav Brain Res 259:143–151. CrossRef Medline

Bissonette GB, Schoenbaum G, Roesch MR, Powell EM (2015) Interneurons are necessary for coordinated activity during reversal learning in orbitofrontal cortex. Biol Psychiatry 77:454–464. CrossRef Medline

Brien JF, Chan D, Green CR, Iqbal U, Gareri J, Kobus SM, McLaughlin BE, Klein J, Rao C, Reynolds JN, Bocking AD, Koren G (2006) Chronic prenatal ethanol exposure and increased concentration of fatty acid ethyl esters in meconium of term fetal Guinea pig. Ther Drug Monit 28:345–350. CrossRef Medline

Centers for Disease Control and Prevention (2012) Alcohol use and binge drinking among women of childbearing age—United States, 2006–2010. Morb Mortal Wkly Rep 61:534–538.

Chang GQ, Karatayev O, Liang SC, Barson JR, Leibowitz SF (2012) Prenatal ethanol exposure stimulates neurogenesis in hypothalamic and limbic peptide systems: possible mechanism for offspring ethanol overconsumption. Neuroscience 222:417–428. CrossRef Medline

Cho KK, Hoch R, Lee AT, Patel T, Rubenstein JL, Sohal VS (2015) Gamma rhythms link prefrontal interneuron dysfunction with cognitive inflexibility in dlx5/6(+/−) mice. Neuron 85:1332–1343. CrossRef Medline

Clancy B, Darlington RB, Finlay BL (2001) Translating developmental time across mammalian species. Neuroscience 105:7–17. CrossRef Medline

Cuzon VC, Yeh PW, Yanagawa Y, Obata K, Yeh HH (2008) Ethanol consumption during early pregnancy alters the disposition of tangentially migrating GABAergic interneurons in the fetal cortex. J Neurosci 28:1854–1864. CrossRef Medline

Fish KN, Hoftman GD, Sheikh W, Kitchens M, Lewis DA (2013) Parvalbumin-containing chandelier and basket cell boutons have distinctive modes of maturation in monkey prefrontal cortex. J Neurosci 33:8352–8358. CrossRef Medline

Flandin P, Zhao Y, Vogt D, Jeong J, Long J, Potter G, Westphal H, Rubenstein JL (2011) Lhx6 and Lhx8 coordinately induce neuronal expression of Shh that controls the generation of interneuron progenitors. Neuron 70:939–950. CrossRef Medline

Fowler SW, Walker JM, Klakotskaia D, Will MJ, Serfozo P, Simonyi A, Schachtman TR (2013) Effects of a metabotropic glutamate receptor 5 positive allosteric modulator, CDPPB, on spatial learning task performance in rodents. Neurobiol Learn Mem 99:25–31. CrossRef Medline

Fryer SL, Tapert SF, Mattson SN, Paulus MP, Spadoni AD, Riley EP (2007) Prenatal alcohol exposure affects frontal-striatal BOLD response during inhibitory control. Alcohol Clin Exp Res 31:1415–1424. CrossRef Medline

Gelman DM, Martini FJ, Nóbrega-Pereira S, Pierani A, Kessaris N, Marín O (2009) The embryonic preoptic area is a novel source of cortical GABAergic interneurons. J Neurosci 29:9380–9389. CrossRef Medline

Gogolla N, Leblanc JJ, Quast KB, Südhof TC, Fagiolini M, Hensch TK (2009) Common circuit defect of excitatory-inhibitory balance in mouse models of autism. J Neurodev Disord 1:172–181. CrossRef Medline

Gogolla N, Takesian AE, Feng G, Fagiolini M, Hensch TK (2014) Sensory integration in mouse insular cortex reflects GABA circuit maturation. Neuron 83:894–905. CrossRef Medline

Green CR, Mihic AM, Nikkel SM, Stade BC, Rasmussen C, Munoz DP, Reynolds JN (2009) Executive function deficits in children with fetal alcohol spectrum disorders (FASD) measured using the Cambridge Neuropsychological Tests Automated Battery (CANTAB). J Child Psychol Psychiatry 50:688–697. CrossRef Medline

Haider B, McCormick DA (2009) Rapid neocortical dynamics: cellular and network mechanisms. Neuron 62:171–189. CrossRef Medline

Hasenstaub A, Shu Y, Haider B, Kraushaar U, Duque A, McCormick DA (2005) Inhibitory postsynaptic potentials carry synchronized frequency information in active cortical networks. Neuron 47:423–435. CrossRef Medline

Hladnik A, Džaja D, Darmopil S, Jovanov-Milošević N, Petanjek Z (2014) Spatio-temporal extension in site of origin for cortical calretinin neurons in primates. Front Neuroanat 8:50. CrossRef Medline

Hunt E, Streissguth AP, Kerr B, Olson HC (1995) Mothers' alcohol con-

sumption during pregnancy: effects on spatial-visual reasoning in 14-year-old children. Psychol Sci 6:339–342. CrossRef

Jiménez D, López-Mascaraque LM, Valverde F, De Carlos JA (2002) Tangential migration in neocortical development. Dev Biol 244:155–169. CrossRef Medline

Kato M, Dobyns WB (2005) X-linked lissencephaly with abnormal genitalia as a tangential migration disorder causing intractable epilepsy: proposal for a new term, "interneuronopathy." J Child Neurol 20:392–397. CrossRef

Kawaguchi Y, Kondo S (2002) Parvalbumin, somatostatin and cholecystokinin as chemical markers for specific GABAergic interneuron types in the rat frontal cortex. J Neurocytol 31:277–287. CrossRef Medline

Kelsom C, Lu W (2013) Development and specification of GABAergic cortical interneurons. Cell Biosci 3:19. CrossRef Medline

Kodituwakku PW, Kalberg W, May PA (2001) The effects of prenatal alcohol exposure on executive functioning. Alcohol Res Health 25:192–198. Medline

Koopmans G, Blokland A, van Nieuwenhuijzen P, Prickaerts J (2003) Assessment of spatial learning abilities of mice in a new circular maze. Physiol Behav 79:683–693. CrossRef Medline

Larkum ME, Nevian T, Sandler M, Polsky A, Schiller J (2009) Synaptic integration in tuft dendrites of layer 5 pyramidal neurons: a new unifying principle. Science 325:756–760. CrossRef Medline

Lavdas AA, Grigoriou M, Pachnis V, Parnavelas JG (1999) The medial ganglionic eminence gives rise to a population of early neurons in the developing cerebral cortex. J Neurosci 19:7881–7888. Medline

Letinic K, Zoncu R, Rakic P (2002) Origin of GABAergic neurons in the human neocortex. Nature 417:645–649. CrossRef Medline

Lewis DA, Curley AA, Glausier JR, Volk DW (2012) Cortical parvalbumin interneurons and cognitive dysfunction in schizophrenia. Trends Neurosci 35:57–67. CrossRef Medline

Long JE, Cobos I, Potter GB, Rubenstein JL (2009) Dlx1&2 and Mash1 transcription factors control MGE and CGE patterning and differentiation through parallel and overlapping pathways. Cereb Cortex 19 [Suppl 1]:i96–i106.

Maier SE, West JR (2001) Drinking patterns and alcohol-related birth defects. Alcohol Res Health 25:168–174. Medline

Marín O, Anderson SA, Rubenstein JL (2000) Origin and molecular specification of striatal interneurons. J Neurosci 20:6063–6076. Medline

Marín O, Rubenstein JL (2001) A long, remarkable journey: tangential migration in the telencephalon. Nat Rev Neurosci 2:780–790. CrossRef Medline

Marquardt K, Sigdel R, Caldwell K, Brigman JL (2014) Prenatal ethanol exposure impairs executive function in mice into adulthood. Alcohol Clin Exp Res 38:2962–2968. CrossRef Medline

Mattson SN, Goodman AM, Caine C, Delis DC, Riley EP (1999) Executive functioning in children with heavy prenatal alcohol exposure. Alcohol Clin Exp Res 23:1808–1815. CrossRef Medline

May PA, Baete A, Russo J, Elliott AJ, Blankenship J, Kalberg WO, Buckley D, Brooks M, Hasken J, Abdul-Rahman O, Adam MP, Robinson LK, Manning M, Hoyme HE (2014) Prevalence and characteristics of fetal alcohol spectrum disorders. Pediatrics 134:855–866. CrossRef Medline

Miyoshi G, Fishell G (2011) GABAergic interneuron lineages selectively sort into specific cortical layers during early postnatal development. Cereb Cortex 21:845–852. CrossRef Medline

Nóbrega-Pereira S, Kessaris N, Du T, Kimura S, Anderson SA, Marín O (2008) Postmitotic Nkx2-1 controls the migration of telencephalic interneurons by direct repression of guidance receptors. Neuron 59:733–745. CrossRef Medline

O'Leary TP, Brown RE (2013) Optimization of apparatus design and behavioral measures for the assessment of visuo-spatial learning and memory of mice on the Barnes maze. Learn Mem 20:85–96. CrossRef Medline

Otsuka T, Kawaguchi Y (2009) Cortical inhibitory cell types differentially form intralaminar and interlaminar subnetworks with excitatory neurons. J Neurosci 29:10533–10540. CrossRef Medline

Parnavelas JG (2000) The origin and migration of cortical neurones: new vistas. Trends Neurosci 23:126–131. CrossRef Medline

Preibisch S, Saalfeld S, Tomancak P (2009) Globally optimal stitching of tiled 3D microscopic image acquisitions. Bioinformatics 25:1463–1465. CrossRef Medline

Price MG, Yoo JW, Burgess DL, Deng F, Hrachovy RA, Frost JD Jr, Noebels JL (2009) A triplet repeat expansion genetic mouse model of infantile spasms syndrome, Arx(GCG)10+7, with interneuronopathy, spasms in infancy, persistent seizures, and adult cognitive and behavioral impairment. J Neurosci 29:8752–8763. CrossRef Medline

Prut L, Belzung C (2003) The open field as a paradigm to measure the effects of drugs on anxiety-like behaviors: a review. Eur J Pharmacol 463:3–33. CrossRef Medline

Ragozzino ME (2007) The contribution of the medial prefrontal cortex, orbitofrontal cortex, and dorsomedial striatum to behavioral flexibility. Ann N Y Acad Sci 1121:355–375. CrossRef

Rasmussen C (2005) Executive functioning and working memory in fetal alcohol spectrum disorder. Alcohol Clin Exp Res 29:1359–1367. CrossRef Medline

Riley EP, McGee CL (2005) Fetal alcohol spectrum disorders: an overview with emphasis on changes in brain and behavior. Exp Biol Med (Maywood) 230:357–365. Medline

Riley EP, Lochry EA, Shapiro NR (1979) Lack of response inhibition in rats prenatally exposed to alcohol. Psychopharmacology 62:47–52. CrossRef Medline

Riley EP, Barron S, Driscoll CD, Hamlin RT (1986) The effects of physostigmine on open-field behavior in rats exposed to alcohol prenatally. Alcohol Clin Exp Res 10:50–53. CrossRef Medline

Riley EP, Infante MA, Warren KR (2011) Fetal alcohol spectrum disorders: an overview. Neuropsychol Rev 21:73–80. CrossRef Medline

Rudy B, Fishell G, Lee S, Hjerling-Leffler J (2011) Three groups of interneurons account for nearly 100% of neocortical GABAergic neurons. Dev Neurobiol 71:45–61. CrossRef Medline

Sadrian B, Wilson DA, Saito M (2013) Long-lasting neural circuit dysfunction following developmental ethanol exposure. Brain Sci 3:704–727. CrossRef Medline

Schneider ML, Moore CF, Adkins MM (2011) The effects of prenatal alcohol exposure on behavior: rodent and primate studies. Neuropsychol Rev 21:186–203. CrossRef Medline

Schonfeld AM, Paley B, Frankel F, O'Connor MJ (2006) Executive functioning predicts social skills following prenatal alcohol exposure. Child Neuropsychol 12:439–452. CrossRef Medline

Shaw CL, Watson GD, Hallock HL, Cline KM, Griffin AL (2013) The role of the medial prefrontal cortex in the acquisition, retention, and reversal of a tactile visuospatial conditional discrimination task. Behav Brain Res 236:94–101. CrossRef Medline

Takada N, Pi HJ, Sousa VH, Waters J, Fishell G, Kepecs A, Osten P (2014) A developmental cell-type switch in cortical interneurons leads to a selective defect in cortical oscillations. Nat Commun 5:5333. CrossRef Medline

Verret L, Mann EO, Hang GB, Barth AM, Cobos I, Ho K, Devidze N, Masliah E, Kreitzer AC, Mody I, Mucke L, Palop JJ (2012) Inhibitory interneuron deficit links altered network activity and cognitive dysfunction in alzheimer model. Cell 149:708–721. CrossRef Medline

Vetreno RP, Crews FT (2012) Adolescent binge drinking increases expression of the danger signal receptor agonist HMGB1 and Toll-like receptors in the adult prefrontal cortex. Neuroscience 226:475–488. CrossRef Medline

Ware AL, Infante MA, O'Brien JW, Tapert SF, Jones KL, Riley EP, Mattson SN (2015) An fMRI study of behavioral response inhibition in adolescents with and without histories of heavy prenatal alcohol exposure. Behav Brain Res 278:137–146. CrossRef Medline

Xu Q, Cobos I, De La Cruz E, Rubenstein JL, Anderson SA (2004) Origins of cortical interneuron subtypes. J Neurosci 24:2612–2622. CrossRef Medline

Xu Q, Tam M, Anderson SA (2008) Fate mapping *Nkx2.1*-lineage cells in the mouse telencephalon. J Comp Neurol 506:16–29. CrossRef Medline

Zhang ZW (2004) Maturation of layer V pyramidal neurons in the rat prefrontal cortex: intrinsic properties and synaptic function. J Neurophysiol 91:1171–1182. CrossRef Medline

Zhao Y, Flandin P, Long JE, Cuesta MD, Westphal H, Rubenstein JL (2008) Distinct molecular pathways for development of telencephalic interneuron subtypes revealed through analysis of Lhx6 mutants. J Comp Neurol 510:79–99. CrossRef Medline